Cytoplasmic Truncation of Glycoprotein Ibα Weakens Its Interaction with von Willebrand Factor and Impairs Cell Adhesion†

Alicia J. Schade, Maneesh Arya, Shan Gao, Reyhan Diz-Küçükkaya, Bahman Anvari, Larry V. McIntire, José A. López, and Jing-fei Dong*

Cox Laboratory for Biomedical Engineering, Rice University, and Thrombosis Research Section, Department of Medicine, and the Department of Molecular and Human Genetics, Baylor College of Medicine, and Veterans Affairs Medical Center, Houston, Texas 77030

Received July 31, 2002; Revised Manuscript Received November 20, 2002

ABSTRACT: The interaction of the platelet glycoprotein (GP) Ib−IX−V complex with von Willebrand factor (VWF) is a critical step in the adhesion of platelets to the subendothelial matrix following endothelial cell damage, particularly under arterial flow conditions. In the human GP Ib−IX−V complex, the recognition of VWF appears to be mediated entirely by GP Ibα, the largest of four GP Ib−IX−V polypeptides. The goal of the present study was to investigate the involvement of the cytoplasmic domain of GP Ibα in the GP Ib−IX−VWF interaction under both static conditions and in the presence of high fluid shear stress. Using Chinese hamster ovary (CHO) cells that express GP Ibβ, GP IX, and either wild-type GP Ibα or GP Ibα mutants missing various lengths of the cytoplasmic domain, we evaluated adhesion and flow-driven cell rolling on immobilized VWF in a parallel-plate flow chamber. Cells expressing GP Ibα polypeptides with truncations of 6−82 amino acids rolled faster than cells expressing wild-type GP Ibα. Cells that expressed polypeptides with intact actin-binding protein 280 binding sites (truncated to residue 582 of 610) rolled more slowly than those expressing GP Ibα with longer truncations. The rolling velocity of cells expressing truncated GP Ibα mutants increased with decreasing VWF coating density. In addition, a fraction of the truncated cells exhibited saltatory translocation at the lower VWF densities. Studies measuring the GP Ibα−VWF bond strength of three of the mutants using laser tweezers showed that progressive deletion of the cytoplasmic domain led to progressive weakening of the strength of individual GP Ibα−VWF bonds.

Platelets play key roles in arresting bleeding and initiating thrombosis in the arterial circulation, where they recognize vessel wall damage while exposed to rapid blood flow and elevated fluid shear stress. The initial adhesion of platelets to the subendothelial matrix is mediated by the interaction of the platelet glycoprotein (GP)[1] Ib−IX−VWF complex with subendothelial von Willebrand factor (VWF) (*1*, *2*). This interaction activates the platelets (*3*), which promotes their aggregation to form a platelet plug with either beneficial (hemostasis) or detrimental (thrombosis) consequences.

The platelet GP Ib−IX−V complex consists of four transmembrane polypeptides: GP Ibα, GP Ibβ, GP IX, and GP V (*4*). Glycoprotein Ibα is the only component of the complex known to bind VWF and also binds thrombin (*5*, *6*), P-selectin (*7*), and leukocyte Mac-1 (*8*). This polypeptide, like the other GP Ib−IX−V complex polypeptides, is a type I transmembrane protein, with the VWF-binding region contained within the most N-terminal 300 amino acids (*4*). This region is followed by a mucin-like region called the macroglycopeptide, a single transmembrane domain, and a cytoplasmic domain of approximately 100 amino acids, through which the complex interacts with the platelet cytoskeleton and signaling proteins (*9*−*12*).

Previous studies (*13*, *14*) have examined the possibility that the cytoplasmic region of GP Ibα may modulate VWF binding. We have previously demonstrated that truncating the cytoplasmic region of GP Ibα increases GP Ib−IX mobility within the plane of the plasma membrane (*13*). The increased mobility correlated with decreased ristocetin-induced VWF binding by cells expressing the mutants at comparable receptor densities, indicating that the anchorage is critical for optimal binding of VWF. In contrast, Cunningham et al. found no difference in botrocetin-induced VWF binding to CHO and melanoma cells expressing cytoplasmic-truncated GP Ibα, but they did observe a change in the pattern of spreading when cells were plated on immobilized VWF (*14*). In support of a role of cytoskeletal attachment in VWF binding, a recent study showed that CHO cells expressing a mutated GP Ibα with its cytoskeleton binding region deleted rolled faster on immobilized VWF under high shear stress conditions compared to cells expressing wild-type GP Ibα (*15*). However, yet another study (*16*) concluded that filamin binding to the GP Ibα cytoplasmic tail negatively influences VWF binding.

† This work was supported by NIH Grants HL02463, HL46416, HL18673, HL65967, and NS23327, Robert A. Welch Foundation Grant C938, a Grant-in-Aid from the American Heart Association−Texas Affiliate, and the NIH Medical Scientist Training Program at Baylor College of Medicine.

* Address correspondence to this author at the Thrombosis Research Section, Department of Medicine, BCM286, N1319, Baylor College of Medicine, One Baylor Plaza, Houston, TX 77030. Telephone: 713-798-3470. Fax: 713-798-3415. E-mail: jfdong@bcm.tmc.edu.

[1] Abbreviations: GP, glycoprotein; VWF, von Willebrand factor; CHO, Chinese hamster ovary cells.

10.1021/bi026549n CCC: $25.00
Published on Web 01/31/2003

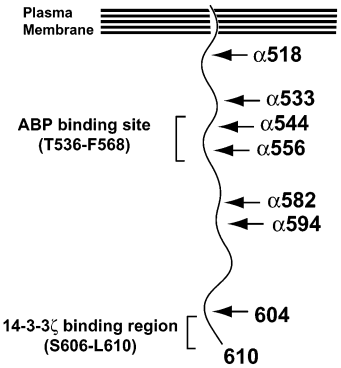

FIGURE 1: Locations of the cytoplasmic truncations. By mutagenesis, seven mutants containing various lengths of truncations in the cytoplasmic domain of GP Ibα were created. The C-terminus mediating interaction of GP Ibα with the intracellular signal protein 14-3-3ζ has been deleted from all of the mutants whereas the region that interacts with the cytoskeleton through actin-binding protein was preserved in three mutants: α582, α594, and α604.

We have previously shown that transfected cells expressing the GP Ib−IX complex adhere to and roll on immobilized VWF in the absence of any other receptor−ligand interaction (*17*). In the current studies, we investigated the relationship between GP Ibα cytoplasmic length and adhesion and translocation on immobilized VWF of mutant-expressing cells exposed to fluid shear stress and compared these results to VWF binding under static conditions induced by modulators. We found that CHO cells expressing mutant GP Ibα polypeptides with truncations of the cytoplasmic domain retained their ability to attach to and roll on immobilized VWF at high shear stress. However, these cells rolled significantly faster than did cells expressing wild-type GP Ibα. These adhesive defects paralleled defects observed in both botrocetin- and ristocetin-induced VWF binding under static conditions. In addition, when we examined single bond strengths with laser tweezers between each of three GP Ibα mutants (truncated after residues 582, 544, and 518), there was a progressive decrease in the single bond strength with increasing cytoplasmic truncation.

EXPERIMENTAL PROCEDURES

Cell Lines. The construction of cell lines expressing truncated GP Ibα polypeptides with wild-type GP Ibβ and GP IX has been described previously (*13*). The truncated GP Ibα polypeptides formed complexes with GP Ibβ and GP IX and expressed at normal levels on the cell membrane (*13*). In the current study, seven such cell lines were employed, expressing GP Ibα with its cytoplasmic domain truncated to various lengths (Figure 1). For example, CHO α604 cells express wild-type GP Ibβ and GP IX with a truncated GP Ibα missing six amino acids from the C-terminus. CHO αβIX cells, expressing wild-type GP Ibα, were used as a positive control, and CHO βIX cells, lacking GP Ibα, were used as a negative control. The cells were grown in α-minimal essential medium (Life Technologies, Grand Island, NY) supplemented with 10% fetal bovine serum (FBS).

Flow Cytometry. Flow cytometry was used for two purposes in these studies. The first was to evaluate the conformation of the truncated mutants by examining their binding to several anti-GP Ibα antibodies: AK2 (RDI, Flanders, NJ), SZ2 (RDI), and WM23 (provided by Michael Berndt, Monash University, Melbourne, Australia). The first two of these antibodies are capable of blocking modulator-induced VWF binding (*18*−*20*). AK2 binds within GP Ibα residues 1−59 and blocks both ristocetin- and botrocetin-induced VWF binding (*20*), SZ2 binds within the anionic sequence Glu268−Asp282 (*21*, *22*), and WM23 binds within the macroglycopeptide and does not interfere with VWF binding (*23*). We also used flow cytometry to determine the surface level of the complex each time the cells were used in rolling experiments. For this, we used SZ2. The preparation and staining of the cells for flow cytometry have been described previously (*18*). Briefly, cells were detached with 0.53 mM EDTA, washed with phosphate-buffered saline (PBS), and incubated with the monoclonal GP Ibα antibodies for 60 min at room temperature followed by an additional 30 min incubation with flourescein isothiocyanate-conjugated rabbit anti-mouse IgG (Zymed, South San Francisco, CA). After unbound antibody was removed by washing with PBS, cell surface expression of wild-type or mutated GP Ibα was measured by flow cytometry on a FACScan flow cytometer (Becton Dickinson, San Jose, CA). Nonspecific binding was determined by the background fluorescence from CHO βIX cells stained with the same antibody. The data were analyzed using Cellquest software from Becton Dickinson.

Modulator-Induced VWF Binding. Purified human VWF (kindly provided by Michael Berndt) was iodinated with $Na^{125}I$ by the Iodogen method and purified on a Sephadex G-25 column (Pharmacia Laboratories, Piscataway, NJ) as described previously (*18*). The specific activity of ^{125}I-labeled VWF was 0.22 mCi/mg of protein. The binding of the radiolabeled ligand was assessed as previously described (*18*). Briefly, CHO cells expressing wild-type or truncated GP Ibα were detached with EDTA and resuspended in Ca^{2+},Mg^{2+}-free Tyrode's buffer to a final concentration of 4×10^6 cells/mL. Twenty-five microliter aliquots of the cell suspension were incubated with increasing concentrations of ^{125}I-VWF and either 20 μg/mL botrocetin (provided by Michael Berndt) or 1.0 mg/mL ristocetin (Sigma) in a total reaction volume of 100 μL. After a 30 min incubation at room temperature, the cells were layered onto a minicolumn containing 20% sucrose to separate membrane-bound VWF from free VWF by centrifugation at 10000*g* for 5 min. The capillary tips of the minicolumn containing the cell pellets were cut off, and the membrane-bound radioactivity was counted in a γ counter. Nonspecific binding was determined by incubating CHO βIX cells with ^{125}I-VWF and modulators. All direct binding data were corrected for nonspecific binding and then normalized for differences in surface levels of the GP Ib−IX−V complex as determined by flow cytometry (*18*).

Preparation of VWF Coverslips. Human VWF was purified from cryoprecipitate by a two-step method of glycine and NaCl precipitation (*24*, *25*) and gel filtration (2.5×50 cm with a 3000 mL bed volume Sepharose 4B column, Pharmacia, Inc.). The VWF was quantified using an enzyme-linked immunoassay (Spectro VWF kit, Ramco Laboratories Inc., Houston, TX) where the concentration of VWF was determined relative to a standard of known VWF concentration. For the flow experiments, the desired VWF concentration (5 or 50 μg/mL) was obtained by diluting the stock VWF solution of known concentration with Dulbecco's PBS

(Sigma Chemical Co.). Next, the diluted VWF solution was coated onto glass coverslips (no. 1, 24 × 50 mm^2; Corning, New York). Previous studies have shown that, within this range of VWF concentration, the amount of protein absorbed on the glass surface increases nonlinearly as the concentration of the protein in the solution increases (*26*). The coverslips were incubated with VWF solution for 45 min at room temperature. Prior to use, the coverslips were rinsed with 10 mL of 0.9% saline. When low-dose VWF was used, the coverslips were then coated with 400 μL of a 2% BSA solution for 2 h at room temperature to block nonspecific binding. Excess BSA was removed by washing with 0.9% NaCl before the parallel-plate flow chamber was assembled.

Parallel-Plate Flow Chamber and Digital Image Processing. The interaction between VWF and the GP Ib−IX−V complex was monitored in a parallel-plate flow chamber placed on an inverted-stage phase-contrast microscope (DIAPHOT-TMD, X-20 phase objective and X-5 projection lens; Nikon, Garden City, NY). The parallel-plate flow chamber consisted of a polycarbonate slab, a silicon gasket (0.015 in.) creating a defined gap, and a glass coverslip coated with VWF. The apparatus was held together by application of a vacuum. The chamber was maintained at 37 °C by an air curtain incubator attached to the microscope. Fluid was drawn through the gap in the chamber by a syringe pump (Harvard Apparatus, Holliston, MA). The wall shear stress created in the chamber is proportional to the fluid viscosity and flow rate and inversely proportional to the width of the chamber and the square of the gap height (*27*, *28*) and was regulated in these experiments through changes in the flow rate. Cells were either injected (500000 cells/mL) into the chamber and allowed to incubate with the immobilized VWF for 1 min or perfused (100000 cells/mL) directly over immobilized VWF without preincubation. The preincubation method was used to increase the probability of cell−protein interactions by allowing the cells to settle on the VWF surface before perfusion. When the association rate of the receptor−ligand interaction was investigated, the cells were perfused through the chamber without preincubation. A lower cell concentration was used in the perfusion method because of limitations in CHO cell quantity.

Images were collected using a silicon-intensified target video camera (Model C2400; Hammatsu, Waltman, MA) attached to the microscope. Subsequently, the images were recorded onto a video cassette. To determine the velocity of cell rolling, the collected images were analyzed off-line on a Sparc Workstation using Inovision digital imaging software (IC-300 Modular Image Processing Workstation; Inovision Corp., Durham, NC). Images that showed the paths traveled by individual cells were obtained by overlapping a set number of images for a determined time interval (i.e., 60 frames/2 s). Only cells that fit the definition of rolling were used in calculating mean rolling velocities. Rolling was defined for these experiments as continuous cell movement in the direction of fluid flow while the cells maintained continuous contact with the immobilized VWF surface for at least 2 s. If the cell rolled a short distance and then returned to the flowing stream and traveled at the fluid velocity for a distance of at least two cell diameters before rolling on the surface a short distance again, the cell was considered to be showing saltatory translocation. A cell showed saltatory movement when it moved at a significantly increased off-rate of the GP Ib−VWF bond. This type of movement represents a transition of cells from rolling to no rolling.

Optical Tweezers and Measurement of Individual GP Ibα−VWF A1 Bond Strengths. The optical tweezers set up and its use to measure GP Ibα−VWF bonds have been described in detail (*29*). In the studies reported here, we used cell lines expressing GP Ib−IX complexes containing either of three GP Ibα truncation mutants, α518, α544, and α582, or expressing wild-type GP Ibα. The optical tweezers were used to trap polystyrene beads coated with the purified recombinant VWF A1 domain (a kind gift of Dr. Miguel Cruz, Baylor College of Medicine), which were then moved into contact with cells expressing the individual mutants by means of a piezoelectric stage (*29*).

Statistics. The cells were analyzed with either Student's *t*-test or the ANOVA *f*-test. Results were reported as means ± SEM.

RESULTS

Antibody Binding to Truncated GP Ibα. To determine if cytoplasmic truncation of GP Ibα affected the conformation of its VWF binding site(s), we analyzed the binding of GP Ibα monoclonal antibodies to the cells. AK2 blocks both ristocetin- and botrocetin-induced VWF binding, and SZ2 selectively blocks botrocetin-induced binding (*18*, *22*). Binding of these two antibodies was normalized to the binding of WM23, a monoclonal antibody that binds within the GP Ibα macroglycopeptide region and which we have previously demonstrated is unaffected by mutations of the cytoplasmic domain (*13*). None of the truncations affected antibody binding (Figure 2A,B), indicating that the conformation of the VWF binding is maintained.

Modulator-Induced VWF Binding. Cells expressing wild-type or truncated GP Ibα were incubated with ^{125}I-VWF in the presence of either botrocetin (20 μg/mL) or ristocetin (1.0 mg/mL) for 30 min at room temperature. Specific binding was determined by subtracting the counts from CHO βIX cells and then correcting for differences in receptor density among the different cell lines. Every mutant bound significantly lower levels of VWF than did the cells expressing wild-type GP Ibα in the presence of botrocetin (25−75% less than CHO αβIX cells, Student's *t*-test, $n = 3$, $p < 0.05$) (Figure 3A). Consistent with previous findings (*13*), cells expressing the truncated mutants also bound less VWF in the presence of ristocetin (60−75% less than CHO αβIX cells, Student's *t*-test, $n = 3$, $p < 0.05$) with CHO βIX/α556 binding the least (Figure 3B).

Rolling of CHO Cells on Immobilized VWF under Shear Conditions. The effect of truncating the cytoplasmic region of GP Ibα on receptor−ligand interactions under high fluid shear stress was evaluated using a parallel-plate flow chamber system. Before incubating the CHO cells in the chamber, we performed flow cytometry to ascertain that all of the cells expressed similar levels of GP Ibα (Figure 2C). The cell suspension was infused into the chamber, and the cells were allowed to settle onto the VWF-coated coverslip (coated with a 50 μg/mL solution of VWF) for 1 min. The chamber was then perfused with buffer to generate a wall shear stress of 10 dyn/cm^2. Under these conditions, all of the mutants rolled on the VWF surface (Figure 4). However, each of the mutants rolled faster than CHO αβIX cells (Student's *t*-test,

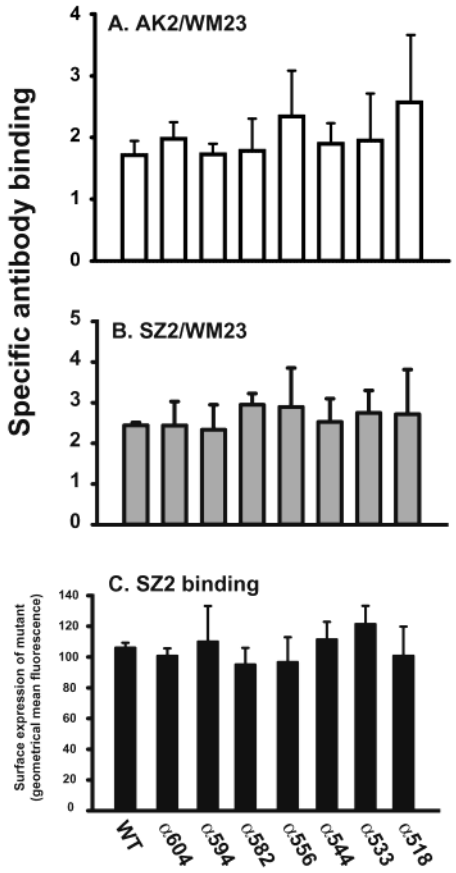

FIGURE 2: Antibody binding to cells expressing truncated GP Ibα. The binding of the GP Ibα antibodies, AK2, SZ2, and WM23, to cells expressing truncated and wild-type GP Ibα was determined by flow cytometry. Specific binding of AK2 and SZ2 was expressed as the ratio to WM23, which serves as a reference antibody because its binding epitope is outside of the ligand-binding domain of GP Ibα. Values are the mean ± SEM, $n = 4$.

$n = 75-300$, $p < 0.001$). The truncations can be divided into two groups: those that preserved the association of GP Ibα with the cytoskeleton (CHO βIX/α604, α594, α582) or eliminated it (CHO βIX/α556, α544, α533) (*10*). The velocities of the second group of cells were significantly higher than that of the first group (Student's *t*-test, $n = 100-300$, $p < 0.001$).

We also evaluated the behavior of the cells on coverslips coated at a much lower VWF density (5 μg/mL coating concentration). This density of VWF supported continuous rolling of all the cell types at a shear stress of 10 dyn/cm^2 (Figure 5) with the rolling velocities of mutant cells again being higher than the velocity of wild-type cells. There were two important differences between cell rolling on high-density VWF and rolling on low-density VWF. First, all of the cell types rolled faster at the lower VWF density (Figure 6A). Comparing to cell rolling on higher VWF density (Figure 4), the velocity increase was greater in the cells expressing truncated GP Ibα that preserved its association with the cytoskeleton so that overall there was no significant difference in velocity among the truncations except for the CHO βIX/α556 cells, which rolled significantly faster than cells expressing other mutants (Student's *t*-test, $n = 70-300$, $p < 0.001$). Second, reducing the VWF concentration resulted in a percentage of cells showing saltatory translocation (Figures 5G and 6B). If the cell rolled a short distance, returned to the flowing stream, and then rolled a short distance again, it was considered to be saltatory translocation.

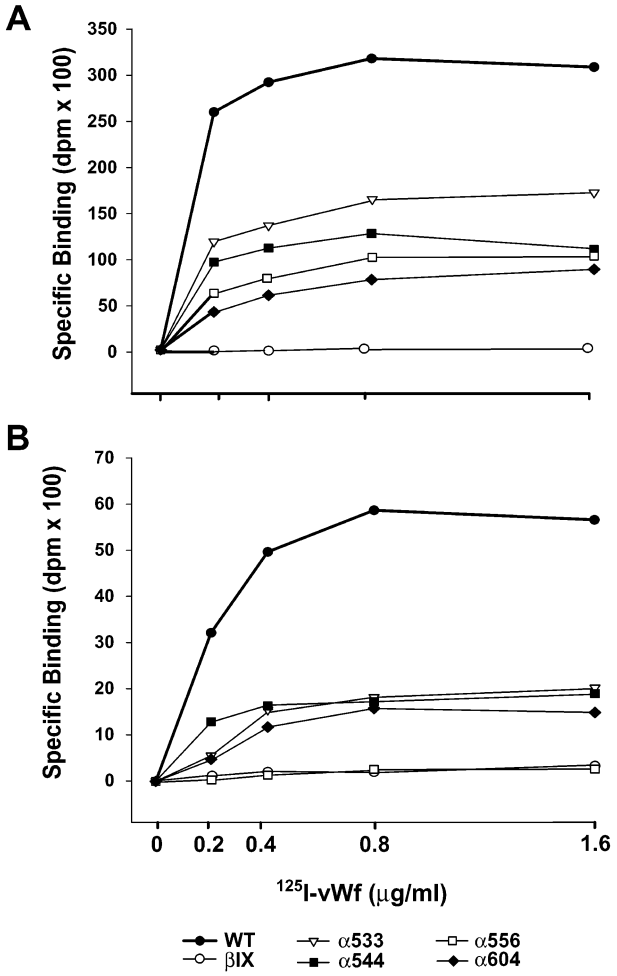

FIGURE 3: Modulator-induced ^{125}I-VWF binding. Binding of ^{125}I-VWF to CHO cells expressing wild-type or truncated GP Ibα was induced in the presence of either 2 μg/mL botrocetin (A) or 1 mg/mL ristocetin (B). Cells expressing a partial complex lacking GP Ibα was used as the negative control. The VWF binding was corrected for nonspecific binding (CHO βIX cells) and surface levels of GP Ibα. Values are a representative of three independent experiments.

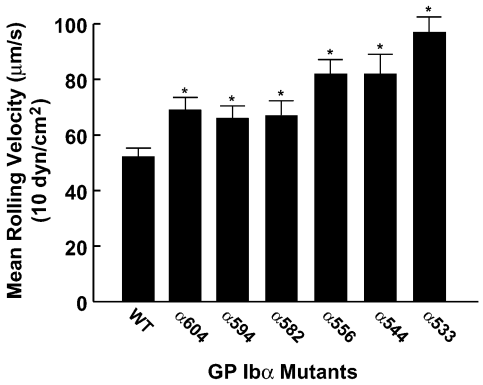

FIGURE 4: Rolling velocity of CHO cells expressing wild-type or truncated GP Ibα on immobilized VWF under flow. Cells were injected into the parallel-plate flow chamber and incubated with immobilized VWF (coating concentration at 50 μg/mL) for 1 min. A steady flow that generated a wall shear stress of 10 dyn/cm^2 was then initiated, and cell rolling recorded real time. Rolling velocity was determined and expressed as micrometers per second. Values are the mean ± SEM, Student's *t*-test, $n = 201-634$ (from three experiments). *$p < 0.05$.

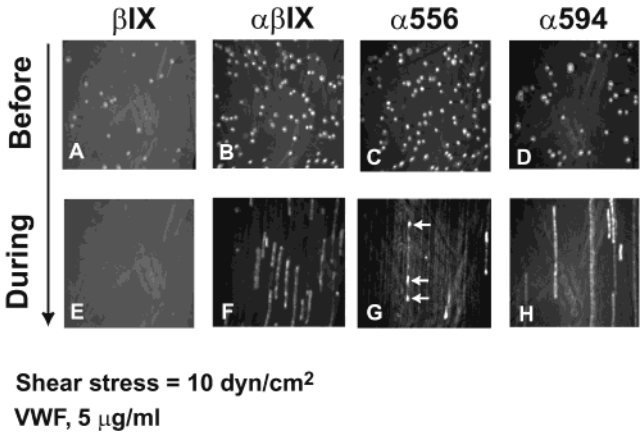

FIGURE 5: Video images of cells expressing truncated GP Ibα rolling on immobilized VWF. Cells were injected into the parallel-plate flow chamber and incubated for 1 min after which the flow was initiated at a wall shear stress of 10 dyn/cm^2. Cell rolling was recorded real time using a VCR and later analyzed off-line using digital imaging software. These video images were created by overlapping 60 frames that resulted in an image that shows the path traveled by the CHO cells during a 2 min period. The top row of images was created during the incubation of the cells in the chamber prior to the initiation of flow. The bottom row of images was created during flow. Arrows indicate positions of temporary rolling of cells exhibiting saltatory translocation between intervals of returning to the flow stream.

The percentage of cells that showed saltatory translocation was greater for all of the cells expressing truncated GP Ibα compared to cells expressing wild-type GP Ibα (ANOVA *f*-test, $n = 200$, $p < 0.001$). The highest percentage of saltating cells was found in cells expressing GP Ibα mutants that disrupted cytoskeletal association.

Effects of Wall Shear Stress on Rolling Velocity of Cells Expressing Truncated GP Ibα. To investigate the ability of the cells to tether to the VWF-coated coverslip from the flow stream, the cells were perfused over immobilized VWF (50 μg/mL) without a prior incubation step. At a wall shear stress of 5 dyn/cm^2, the wild-type and truncated GP Ibα cells tethered to the VWF surface and then exhibited continuous rolling on the surface (data not shown). All the cells expressing truncated GP Ibα rolled faster than cells expressing wild-type GP Ibα with CHO βIX/α556 cells rolling significantly faster than the other mutants (Student's *t*-test, $n = 70-100$, $p < 0.001$).

We also examined the effect of wall shear stress by performing a shear titration study at wall shear stresses of 5, 10, or 15 dyn/cm^2. The rolling velocities of cells expressing wild-type GP Ibα did not increase with an increase in shear stress from 5 to 10 dyn/cm^2 (Figure 7) but almost doubled with a further increase to 15 dyn/cm^2 (Student's *t*-test, $n = 25-60$, $p < 0.001$). The rolling velocities of cells expressing truncated GP Ibα fell into two patterns. The rolling velocity of those cells in which the cytoskeletal association was maintained (CHO βIX/α604 and CHO βIX/α582) increased dramatically when the wall shear stress increased from 5 to 10 dyn/cm^2 (Student's *t*-test, $n = 70-300$, $p < 0.001$) but did not increase further when the shear stress was increased to 15 dyn/cm^2 (Figure 7). In contrast, cells expressing truncations that eliminated the cytoskeleton association of GP Ibα (CHO βIX/α544 and CHO βIX/α533) showed no significant change when wall shear stress increased from 5 to 15 dyn/cm^2 (Figure 7).

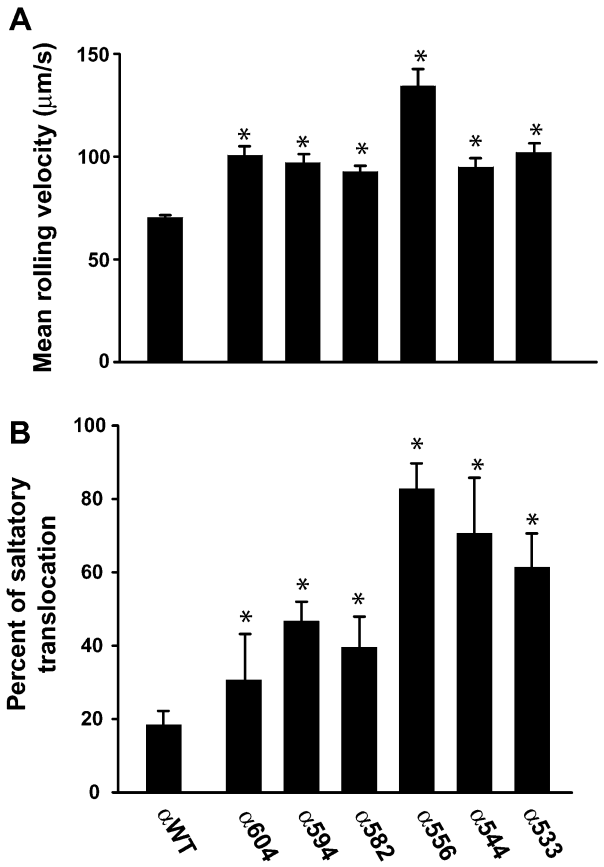

FIGURE 6: Rolling velocity of CHO cells expressing wild-type or truncated GP Ibα on low density of immobilized VWF. Cells were injected into the parallel-plate flow chamber and incubated for 1 min on coverslips coated with a solution of 5 μg/mL VWF. Flow was then initiated at a wall shear stress of 10 dyn/cm^2. Rolling velocity was determined for cells that exhibited continuous rolling (A). Values are the mean of 22−376 cells from three to five experiments for each data point with SEM error bars, Student's *t* test. *$p < 0.001$. Percentage of cells that showed saltatory translocation was also determined (B). Values are the mean of three to five experiments for each data point with SEM error bars, Student's *t*-test. *$p < 0.001$.

Bond Strength Measurement Using Optical Tweezers. There are at least two possibilities for our findings thus far: that the diminished interaction of GP Ibα with VWF is a consequence of decreased lateral association of complexes (an effect on topology) or that it results from an effect of the truncation on the ability of individual polypeptide chains to interact with VWF. To discern between these possibilities, we examined the bond strengths between the VWF A1 domains and three truncation mutants (α582, α544, and α518) using optical tweezers. Progressive truncation of the GP Ibα cytoplasmic domain progressively diminished the bond strength, with values for minimal bonds (in picoNewtons) of 11.5 ± 0.4, 8.25 ± 0.9, 6.8 ± 1.0, and 6.1 ± 0.5, respectively, for wild-type GP Ibα, α582, α544, and α518, respectively (Figure 8). There was no measurable binding of VWF beads to CHO βIX cells.

DISCUSSION

Previous studies have shown that truncating the cytoplasmic domain of GP Ibα decreased the binding of soluble VWF induced by ristocetin (*13*) but not by botrocetin (*14*). The primary focus of our current study was to determine whether

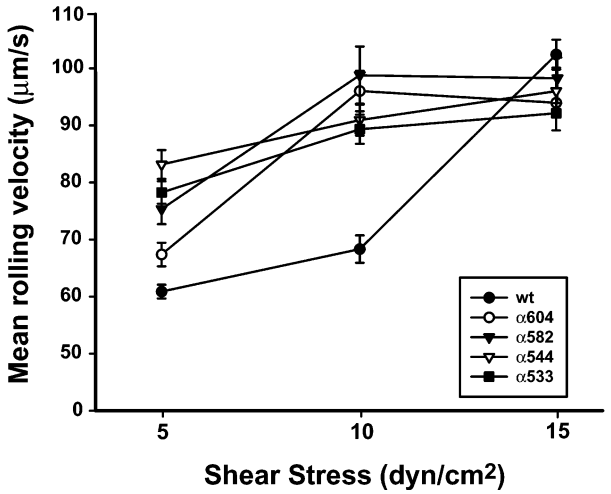

FIGURE 7: Cell rolling under different fluid shear stresses. CHO cells expressing wild-type or truncated GP Ibα were directly perfused over immobilized VWF under shear stress of either 5, 10, or 15 dyn/cm^2. Cell rolling was recorded real time and analyzed for rolling velocity off-line. Values are the mean of 100−300 cells from three experiments for each data point with SEM error bars.

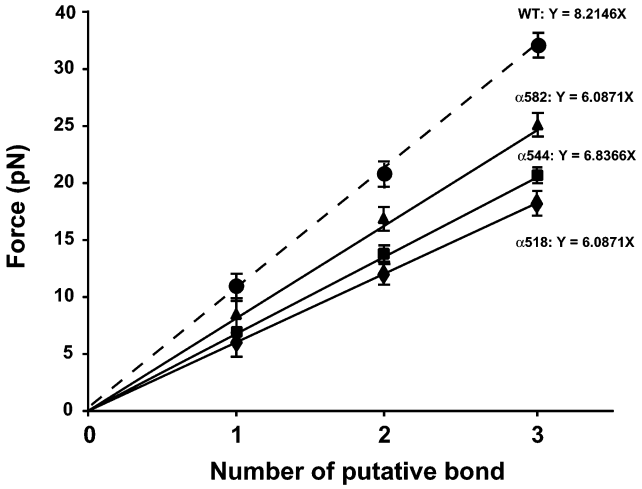

FIGURE 8: Strength of the bond between VWF A1 and GP Ibα. Polystyrene beads coated with the recombinant VWF A1 protein were allowed to briefly contact CHO cells expressing either wild-type or truncated GP Ibα, and the strength of the GP Ibα−VWF bond was then determined by measuring forces required to remove beads from cells. The bond strength was expressed as picoNewtons. The figure is representative of 30 measurements.

truncating the cytoplasmic domain of GP Ibα also affects the interaction between the GP Ib−IX−V complex and VWF under fluid shear stress and to determine if these changes in association rates induced by cytoplasmic truncation are reflected in changes in the strength of individual GP Ibα-VWF bonds. We evaluated seven CHO cell lines with GP Ibα truncations of 6−82 amino acids from the C-terminus and found that they were all able to adhere to and roll on a VWF surface when first allowed to settle on the surface. The cells adhered to a surface coated with two different VWF concentrations (5 and 50 μg/mL) and at three different shear stresses (5, 10, and 15 dyn/cm^2). The mean rolling velocities of the mutant cells were significantly higher than that of wild-type cells (Figures 4−6), consistent with the mutations increasing the off-rate of the GP Ibα−VWF interaction. Consistent with this result, Cranmer et al. recently showed that CHO cells expressing GP Ibα with deletion of 535−586 within the cytoplasmic domain rolled 50% faster than CHO cells expressing wild-type GP Ibα at a shear rate of 3000 s^{-1} (*15*).

We also examined whether truncating the GP Ibα cytoplasmic domain altered the ability of the cells to attach to the VWF matrix from the bulk flow (a parameter related to the on-rate). For this, the cells were directly perfused over the immobilized VWF without first being allowed to settle on the matrix. Cells expressing the truncated GP Ibα attached as efficiently as did cells expressing wild-type GP Ibα, an indication that the on-rate was similar. Once attached, the cells exhibited the same pattern of increased rolling velocity as in the preincubation experiments. Together, the data indicate that truncation of the GP Ibα cytoplasmic domain primarily increases the off-rate of the GP Ibα−VWF bond.

Although the precise mechanism by which the GP Ibα cytoplasmic domain influences the ligand-binding function of the GP Ib−IX−V complex remains to be determined, earlier studies may provide some clues. Two regions within this domain have been shown to interact with cytoplasmic molecules, the region spanning Thr536−Phe568, which binds the cytoskeletal protein actin-binding protein 280 (ABP-280), and the terminal five residues, known to interact with the 14-3-3ζ signaling protein (*10*, *12*, *30*). That both sites are important for anchoring the complex in a relatively fixed position on the plasma membrane was demonstrated by our studies employing the technique of fluorescence recovery after photobleaching (*13*). Truncations of as few as five residues from the GP Ibα C-terminus greatly increased the mobility of the complex on the cell surface, and the mobility was increased further with larger truncations. The change in lateral mobility of the complex could affect its ligand binding function in at least two ways. First, the mobility change could affect the formation of a functional receptor. Previous studies have shown that a functional receptor for VWF may consist of more than one GP Ib−IX complex (*31*), and receptor function may depend on the association of the complex with the cytoskeleton. A functional receptor may be less likely to form among GP Ib−IX−V complexes that are highly mobile. Second, the increased mobility could change the arrangement of GP Ib−IX complexes on the cell surface, a determinant that may allow the attachment of multiple complexes to a single VWF multimer, which contains multiple GP Ibα binding sites. Since the multiple VWF A1 domains (the GP Ibα-binding domain of VWF) in a VWF multimer are likely to be spaced evenly, they may require the GP Ib−IX−V complex to be arranged in such geometry on the cell surface that it can receive the ligand optimally. Thus, disruption of the fixed receptor array could affect ligand binding.

Alternatively, the decreased ligand binding associated with GP Ibα cytoplasmic truncation could be unrelated to changes in complex mobility. For example, the truncation could affect the conformation of the GP Ibα VWF binding site. We consider this possibility unlikely because a host of conformation-sensitive antibodies bind normally to cells expressing the mutants. These antibodies have been shown to block modulator-induced VWF binding (*18*, *22*), and one antibody, AK2, has also been shown to block the rolling of cells expressing the GP Ib−IX−V complex on immobilized VWF (*17*). The optical tweezer data suggest a possible effect of the truncation on the positioning of the GP Ibα N-terminus for optimal

binding, as progressive truncation of the cytoplasmic domain also progressively decreased the bond strength between the VWF A1 domain and GP Ibα. The fact that the truncation did not produce stepwise changes in bond strength (e.g., reducing the bond strength by quarter- or half-steps) argues against a change in complex stoichiometry induced by the truncations. These studies contrasted with the flow chamber studies in that the latter involved the effect of shear stress on the bonds. Another possibility is that the truncations disrupt signaling pathways that could be required for reinforcing ligand binding. There is ample recent evidence that the GP Ibα cytoplasmic domain mediates transmembrane signaling (*3*, *32*, *33*), a process that involves 14-3-3ζ (*34*−*36*).

We also evaluated the effect of truncating the cytoplasmic region GP Ibα on botrocetin-induced VWF binding using CHO cells expressing the various truncated GP Ibα mutants. All of the mutants displayed decreased botrocetin-induced VWF binding compared to wild-type cells, similar to our earlier results examining ristocetin-induced binding. This result is at odds with the findings of Cunningham et al. (*14*), who found no difference in botrocetin-induced VWF binding between cells expressing wild-type GP Ibα and cells expressing a mutant truncated after residue Gln545. Our results on ristocetin-induced VWF binding to the truncation mutants are also different from those of Englund et al. (*16*), who found that binding of soluble VWF to the GP Ib-IX complexes was enhanced when interaction between the cytoplasmic domain of GP Ibα and the cytoskeleton was disrupted by either cytochalasin D treatment or cytoplasmic truncations. One notable difference between our studies and those of Cunningham et al. (*14*) and Englund et al. (*16*) is that in our studies VWF binding was evaluated with equilibrium binding of radiolabeled VWF, whereas in the other two studies VWF binding to the cells was assessed by flow cytometry. Cytometric analysis requires removal of the soluble VWF and incubation with the VWF antibody before analysis. This allows the reversibly bound VWF to detach from the cells, while a more tightly bound component would remain. In the studies employing radiolabeled VWF, by contrast, the separation of the bound from the free VWF is instantaneous as the cells are centrifuged through the sucrose cushion. Thus, it is possible that the truncations differentially affect different components of VWF binding, a reversible equilibrium component and a component of markedly increased affinity. Our data indicate that the former component of VWF binding correlates more closely with the strength of the GP Ibα−VWF bond and with the dynamics of the interaction under flow. It is interesting to observe that Williamson et al. (*37*) demonstrated an increase in the rolling velocity of cells that express cytoplasmic truncations. These same cells have previously been shown by the same group to enhance VWF binding when treated with cytochalasin D (*38*).

In summary, the cytoplasmic domain of GP Ibα is important in GP Ib−IX−VWF interaction under both static and flow conditions, modulating the strength of the bond between receptor and ligand.

REFERENCES

1. Andrews, R. K., López, J. A., and Berndt, M. C. (1997) *Int. J. Biochem. Cell Biol. 29*, 91−105.
2. Berndt, M. C., Shen, Y., Dopheide, S. M., Gardiner, E. E., and Andrews, R. K. (2001) *Thromb. Haemostasis 86*, 178−188.
3. Kroll, M. H., Hellums, J. D., McIntire, L. V., Schafer, A. I., and Moake, J. L. (1996) *Blood 88*, 1525−1541.
4. Lopez, J. A. (1994) *Blood Coagulation Fibrinolysis 5*, 97−119.
5. Berndt, M. C., and Phillips, D. R. (1981) *Ann. N.Y. Acad. Sci. 370*, 87−95.
6. Li, C. Q., Vindigni, A., Sadler, J. E., and Wardell, M. R. (2001) *J. Biol. Chem. 276*, 6161−6168.
7. Romo, G. M., Dong, J. F., Schade, A. J., Gardiner, E. E., Kansas, G. S., Li, C. Q., McIntire, L. V., Berndt, M. C., and Lopez, J. A. (1999) *J. Exp. Med. 190*, 803−814.
8. Simon, D. I., Chen, Z., Xu, H., Li, C. Q., Dong, J., McIntire, L. V., Ballantyne, C. M., Zhang, L., Furman, M. I., Berndt, M. C., and Lopez, J. A. (2000) *J. Exp. Med. 192*, 193−204.
9. Andrews, R. K., and Fox, J. E. B. (1991) *J. Biol. Chem. 266*, 7144−7147.
10. Andrews, R. K., and Fox, J. E. B. (1992) *J. Biol. Chem. 267*, 18605−18611.
11. Du, X., Harris, S. J., Tetaz, T. J., Ginsberg, M. H., and Berndt, M. C. (1994) *J. Biol. Chem. 269*, 18287−18290.
12. Du, X., Fox, J. E., and Pei, S. (1996) *J. Biol. Chem. 271*, 7362−7367.
13. Dong, J. F., Li, C. Q., Sae-Tung, G., Hyun, W., Afshar-Kharghan, V., and Lopez, J. A. (1997) *Biochemistry 36*, 12421−12427.
14. Cunningham, J. G., Meyer, S. C., and Fox, J. E. (1996) *J. Biol. Chem. 271*, 11581−11587.
15. Cranmer, S. L., Ulsemer, P., Cooke, B. M., Salem, H. H., de la Salle, C., Lanza, F., and Jackson, S. P. (1999) *J. Biol. Chem. 274*, 6097−6106.
16. Englund, G. D., Bodnar, R. J., Li, Z., Ruggeri, Z. M., and Du, X. (2001) *J. Biol. Chem. 276*, 16952−16959.
17. Fredrickson, B. J., Dong, J. F., McIntire, L. V., and Lopez, J. A. (1998) *Blood 92*, 3684−3693.
18. Dong, J. F., Li, C. Q., and Lopez, J. A. (1994) *Biochemistry 33*, 13946−13953.
19. Dong, J. F., Berndt, M. C., Schade, A., McIntire, L. V., Andrews, R. K., and Lopez, J. A. (2001) *Blood 97*, 162−168.
20. Shen, Y., Romo, G. M., Dong, J. F., Schade, A., McIntire, L. V., Kenny, D., Whisstock, J. C., Berndt, M. C., Lopez, J. A., and Andrews, R. K. (2000) *Blood 95*, 903−910.
21. Ward, C. M., Andrews, R. K., Smith, A. I., and Berndt, M. C. (1996) *Biochemistry 35*, 4929−4938.
22. Dong, J., Ye, P., Schade, A. J., Gao, S., Romo, G. M., Turner, N. T., McIntire, L. V., and Lopez, J. A. (2001) *J. Biol. Chem. 276*, 16690−16694.
23. Berndt, M. C., Du, X., and Booth, W. J. (1988) *Biochemistry 27*, 633−640.
24. Thorell, L., and Blomback, B. (1984) *Thromb. Res. 35*, 431−450.
25. Moake, J. L., Turner, N. A., Stathopoulos, N. A., Nolasco, L. H., and Hellums, J. D. (1986) *J. Clin. Invest. 78*, 1456−1461.
26. Moroi, M., Jung, S. M., Nomura, S., Sekiguchi, S., Ordinas, A., and Diaz-Ricart, M. (1997) *Blood 90*, 4413−4424.
27. Bird, R. B., Stewart, W. E., and Lightfoot, E. N. (1960) in *Transport Phenomena*, Wiley, New York.
28. Slack, S. M., and Turitto, V. T. (1994) *Thromb. Haemostasis 72*, 777−781.
29. Arya, M., Anvari, B., Romo, G. M., Cruz, M. A., Dong, J. F., McIntire, L. V., Moake, J. L., and Lopez, J. A. (2002) *Blood 99*, 3971−3977.
30. Andrews, R. K., Harris, S. J., McNally, T., and Berndt, M. C. (1998) *Biochemistry 37*, 638−647.
31. Lopez, J. A., and Dong, J. F. (1997) *Curr. Opin. Hematol. 4*, 323−329.
32. Christodoulides, N., Feng, S., Resendiz, J. C., Berndt, M. C., and Kroll, M. H. (2001) *Thromb. Res. 102*, 133−142.
33. Bodnar, R. J., Gu, M., Li, Z., Englund, G. D., and Du, X. (1999) *J. Biol. Chem. 274*, 33474−33479.
34. Feng, S., Christodoulides, N., Resendiz, J. C., Berndt, M. C., and Kroll, M. H. (2000) *Blood 95*, 551−557.
35. Gu, M., Xi, X., Englund, G. D., Berndt, M. C., and Du, X. (1999) *J. Cell Biol. 147*, 1085−1096.
36. Gu, M., and Du, X. (1998) *J. Biol. Chem. 273*, 33465−33471.
37. Williamson, D., Pikovski, I., Cranmer, S. L., Mangin, P., Mistry, N., Domagala, T., Chehab, S., Lanza, F., Salem, H. H., and Jackson, S. P. (2002) *J. Biol. Chem. 277*, 2151−2159.
38. Mistry, N., Cranmer, S. L., Yuan, Y., Mangin, P., Dopheide, S. M., Harper, I., Giuliano, S., Dunstan, D. E., Lanza, F., Salem, H. H., and Jackson, S. P. (2000) *Blood 96*, 3480−3489.

BI026549N